

Rotor Fault Detection and Identification on a Hexacopter Based on Statistical Time Series Methods

Airin Dutta
PhD Student

Michael McKay
PhD Student

Fotis Kopsaftopoulos
Assistant Professor

Farhan Gandhi
Redfern Professor
Director

Center for Mobility with Vertical Lift (MOVE)
Rensselaer Polytechnic Institute, Troy, NY

ABSTRACT

This work introduces the use of statistical time series methods to detect rotor failures in multicopters. A concise overview of the development of various time series models using scalar or vector signals, statistics, and fault detection methods is provided. The fault detection methods employed in this study are based on parametric time series representations and response-only signals of the aircraft state, as the external excitation is non-observable. The comparative assessment of the effectiveness of scalar and vector statistical models and several residual-based fault detection methods are presented in the presence of external disturbances, such as various levels of turbulence and uncertainty, and for different rotor failure scenarios. The results of this study demonstrate the effectiveness of all the proposed residual-based time series methods in terms of prompt rotor fault detection, although the methods based on Vector Autoregressive (VAR) models exhibit improved performance compared to their scalar counterparts with respect to their robustness and effectiveness for different turbulence levels and ability to distinguish between healthy and fault compensated condition after rotor failure.

NOTATION

α	:	Type I risk level
β	:	Type II risk level
γ	:	Autocorrelation
τ	:	Lag
σ^2	:	Residual variance
Σ	:	Residual covariance matrix
ARMA	:	AutoRegressive Moving Average
$E\{\cdot\}$:	Expected value
PE	:	Prediction Error
ARX	:	AutoRegressive with eXogenous excitation
PSD	:	Power Spectral Density
BIC	:	Bayesian Information Criterion
RSS	:	Residual Sum of Squares
FRF	:	Frequency Response Function
ACF	:	Auto-Covariance Function
iid	:	identically independently distributed
SPP	:	Samples Per Parameter
LS	:	Least Squares
SPRT	:	Sequential Probability Ratio Test
SSS	:	Signal Sum of Squares
AR	:	Scalar AutoRegressive model
VAR	:	Vector AutoRegressive model

INTRODUCTION

Multicopters, being capable of hovering and vertical take-off and landing, have attracted the interest of the community with respect to both commercial and defense applications over the last decade. Given the increasing interest and widespread use of these vehicles in a number of important arenas, early fault detection and identification of such systems are critical in order to ensure and improve their overall safety and reliability.

Rotorcraft are complex systems that exhibit strong dynamic coupling between rotors, fuselage, and control inputs, as well as time-varying and cyclo-stationary behavior. As a result, they face certain system modeling and fault detection and identification challenges that are not present in fixed-wing aircraft. These issues, as well as potential solutions, have been explored in the recent literature.

An algorithm for online detection of motor failure using only inertial measurements and control allocation by an exact redistributed pseudo-inverse method for octacopters has been demonstrated by Frangenberg et al. (Ref. 1). Heredia and Ollero (Ref. 2) have addressed sensor fault identification in small autonomous helicopters using Observer/Kalman Filter identification. Fault tolerant control for multi-rotors (Refs. 3,4), as well as various fault diagnosis methods such as analytical models, signal processing, and knowledge-based approaches for helicopters have also been proposed (Ref. 5).

Statistical time series methods have been used to detect various fault types in aircraft control systems due to their simplicity, efficient handling of uncertainties, no requirement of physics based models, and applicability to different operating conditions (Refs. 6–9). Dimogianopoulos et al. (Ref. 10)

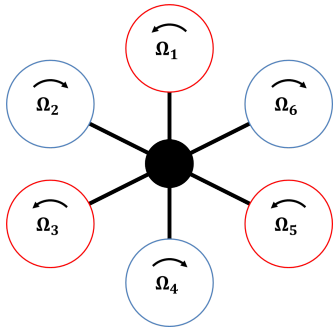


Fig. 1. Schematic representation of a regular hexacopter

have demonstrated the effectiveness of two statistical schemes based on Pooled Non-Linear AutoRegressive Moving Average with eXogenous excitation (P-NARMAX) to detect and isolate faults for aircraft systems under different flight conditions, turbulence levels, and fault types and magnitudes. The first method models the pilot input and aircraft pitch rate relationship, while the second approach models the relationship between horizontal and vertical acceleration, angle of attack and pitch rate signals in fixed-wing aircraft.

The objective of the present study is the development of a robust framework for fault detection in multicopters using statistical time series methods to achieve early detection of rotor failures in the presence of external disturbances, such as turbulence, and uncertainty. This information will be extremely useful for control allocation redistribution and reconfiguration of the vehicle to accomplish safe flight.

HEXACOPTER MODEL AND DATA GENERATION

Physics-Based Modeling of Multicopter System

A flight simulation model has been developed for a regular hexacopter (Fig. 1) using summation of forces and moments to calculate aircraft accelerations. This model is used as the main source of simulated data under varying operating and environmental conditions, as well as different fault types. Rotor loads are calculated using Blade Element Theory coupled with a 3×4 Peters-He finite state dynamic wake model (Ref. 11). This model allows for the simulation of abrupt rotor failure by ignoring the failed rotor inflow states and setting the output rotor forces and moments to zero.

A feedback controller is implemented on the nonlinear model to stabilize the aircraft altitude and attitudes, as well as track desired trajectories written in terms of the aircraft velocities. This controller is designed at multiple trim points, with gain scheduling between these points to improve performance throughout the flight envelope.

The state vector consists of the 12 rigid body states and is defined in Eq. 1.

$$\mathbf{x} = \{X \ Y \ Z \ \phi \ \theta \ \psi \ u \ v \ w \ p \ q \ r\}^T \quad (1)$$

The input vector is comprised of the first four independent multicopter controls for collective, roll, pitch and yaw and is

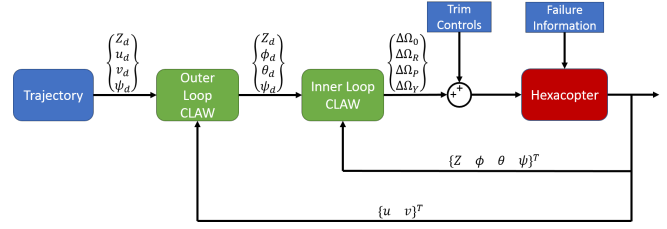


Fig. 2. Controller Block Diagram

defined in Eq. 2:

$$\mathbf{u} = \{\Omega_0 \ \Omega_R \ \Omega_P \ \Omega_Y\}^T \quad (2)$$

The control architecture is illustrated in Fig. 2 and detailed in Ref. 3. This control design has been demonstrated to perform well even in the event of rotor failure, with no adaptation in the control laws themselves.

Data Generation for Model Identification

A continuous Dryden wind turbulence model (Ref. 12) has been implemented in the flight simulation model. The Dryden model is dependent on altitude, length scale, and turbulence intensity and outputs the linear and angular velocity components of continuous turbulence as spatially varying stochastic signals. The proper combination of these parameters determines the fit of the signals to observed turbulence.

In this system, altitude is taken as 5m and the length scale as the hub-to-hub distance of the hexacopter, which is equal to 0.6096 m (2 ft). The data sets for aircraft states are generated through a series of simulations for different turbulence levels (light, moderate and severe) both for healthy aircraft and different fault types, such as failure of front and side rotors. For a summary of the generated data sets see Table 1. The time series (signals) of the hexacopter attitudes (aircraft states) for the healthy state, as well as for different fault types, i.e. complete failure of front rotor or side rotor, provide useful insight into the dynamics of the system. The rotor failures addressed in this work are: front rotor (rotor 1), right-side rotor (rotor 2), and left-side rotor (rotor 6).

Workframe of Statistical Time Series for Fault Detection

Let Z_o designate the aircraft under consideration in its healthy state, and Z_A, Z_B, \dots the aircraft under fault of type A, B, \dots

Table 1. Simulation Data

Aircraft state	number of datasets for turbulence levels		
	Light	Moderate	Severe
Healthy	20	20	20
Rotor failure (1)	20	20	20
Rotor failure (2)	20	20	20
Rotor failure (6)	20	20	20
Sampling frequency: $f_s = 1000$ Hz			
Signal length in samples: 60000 (60 s)			

and so on. Z_u designates the unknown (to be determined) state of the aircraft. Statistical time series modeling is based on discretized response signals $y[t]$ ¹ (for $t = 1, 2, \dots, N$) which are the aircraft states. N denotes the number of samples and the conversion from discrete normalized time to analog time is based on $(t - 1)T_s$, with T_s being the sampling period. The response signals are represented by Z and subscript (o, A, B, \dots, u) is used to denote the corresponding state of the aircraft that produced the signals. The sampling frequency (F_s) for the signals is chosen such that the frequency range of interest is 0 – 500 Hz.

The signals generated from simulation are analyzed by parametric or non-parametric statistical time series methods and proper models are fitted and validated. Such models are identified for the cases Z_o, Z_A, Z_B, \dots in the baseline phase. Fault detection is based on binary statistical hypothesis testing (Ref. 13) that compares the residual properties generated from Z_u in each inspection phase with that available from baseline models. The design of a binary statistical hypothesis test is generally based on the probabilities of type I (false alarm) and type II (missed faults) error probabilities, represented by α and β respectively.

The general workframe for fault detection and identification via statistical time series modeling is illustrated in Fig. 3. Note that in the current study only the task of fault detection is addressed. The task of fault identification (classification) is the topic of current research and will be presented in a future study.

BASELINE MODELING OF THE HEALTHY AIRCRAFT

The aircraft signals for roll, pitch and yaw attitudes generated via a series of simulations of forward flight of the hexacopter under turbulence (light, moderate and severe levels) for healthy and different faulty states are used for model identification and fault detection.

In the present scenario, the signals obtained are response only signals with the excitation $x[t]$ assumed to be a white (uncorrelated) signal induced by atmospheric turbulence. That is $\gamma_{xx}[\tau] = 0$ for $\tau \neq 0$, where γ_{xx} denotes the AutoCorrelation Function (ACF) and τ the ACF time lag, given as:

$$\gamma_{xx}[\tau] = E\{x[t] \cdot x[t + \tau]\} \quad (3)$$

Non-parametric Identification and Fault Detection

Short-Time Fourier Transform or Spectrogram

The Short-time Fourier Transform (STFT) of a discrete-time signal is defined via a moving window as follows:

$$Y[n, \omega] = \sum_{m=0}^{L-1} y[n+m] \cdot w[m] \cdot e^{-i2\pi km/N} \quad (4)$$

¹A functional argument in parentheses designates function of a real variable; for instance $x(t)$ is a function of analog time $t \in R$. A functional argument in brackets designates function of an integer variable; for instance $x[t]$ is a function of normalized discrete time ($t = 1, 2, \dots$).

where n denotes the location in time, L denotes the length of the window (w), and ω the frequency. The square of the magnitude of the STFT yields the spectrogram:

$$S[n, \omega] = |Y[n, \omega]|^2 \quad (5)$$

Spectrogram gives the power intensity of the frequencies present for a particular time window. With sliding windows over time, it is possible to detect changes in the frequency of the signal, which can provide a preliminary idea on the dynamic content and transient effects due to the existence of faults.

Parametric Identification via Time Series Models

Scalar AR Identification Method

A single signal obtained from a healthy flight simulation is parametrized to form a scalar (univariate) AutoRegressive time series model (Ref. 14):

$$y[t] + \sum_{i=1}^{na} a_i \cdot y[t-i] = e[t], \quad e[t] \sim iid N(0, \sigma_e^2) \quad (6)$$

with a_i and na designating the AR parameters and model orders respectively, iid stands for identically independently distributed, and $N(\cdot, \cdot)$ denotes a univariate normal distribution with the indicated mean and variance, respectively. In Eq. 6, $e[t]$ coincides with the one-step-ahead-prediction error and is also referred as the model residual sequence or innovations (Refs. 14, 15).

The identification of parametric time series models is comprised of two main tasks: parameter estimation and model order selection. The parameters for the AR model can be estimated by minimization of the Least Squares (LS) criterion (Refs. 15, 16), whereas the model order selection is achieved based on the examination of the Bayesian Information Criterion (BIC) (Refs. 15, 16) (Eq. 7) and Residual sum of Squares over Signal Sum of Squares Criterion (RSS/SSS) (Eq. 8). The former is a statistical criterion that penalizes model complexity (order, and hence the number of free parameters) as a counteraction to a decreasing model fit criterion. The latter determines the predictive capability of the model.

$$BIC = \ln \sigma_e^2 + (d \times \ln N)/N \quad (7)$$

$$RSS/SSS = \frac{\sum \sigma_e^2}{\sum y[t]^2} \quad (8)$$

In Eq. 7, σ_e^2 is the variance of the residuals, d denotes the number of parameters to be estimated for the model and N denotes the number of samples used for estimation.

Vector AR Identification Method

Vector AutoRegressive (VAR) models employ s -dimensional signals, i.e. the aircraft states in the present study, for multivariate (s -variate) time series modeling (Refs. 17, 18). Though they bear striking resemblance to their univariate or scalar

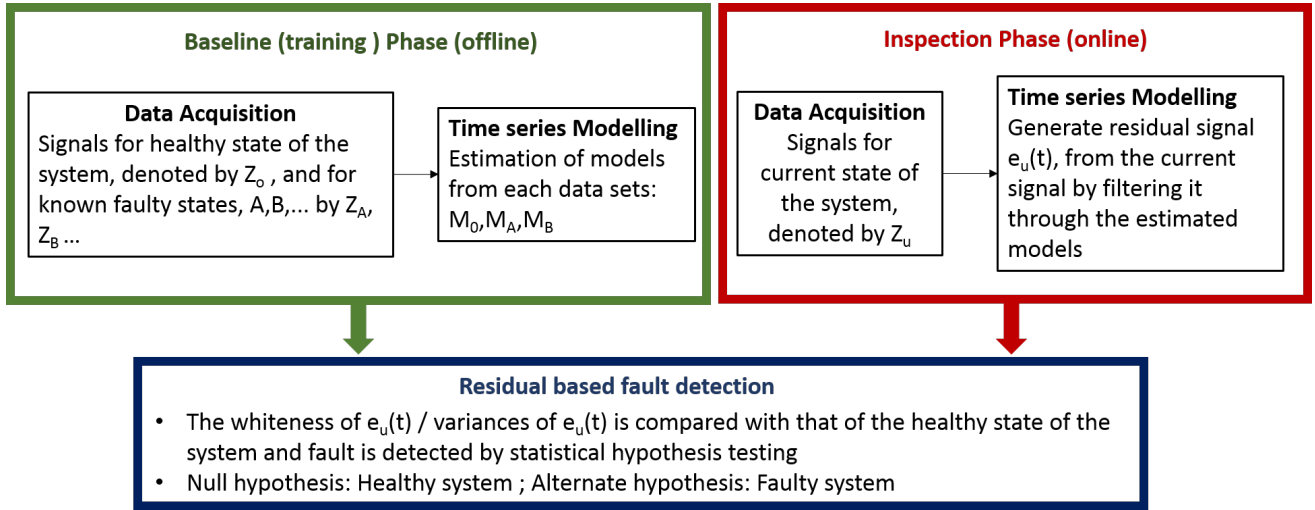


Fig. 3. General workframe of statistical time series methods for fault detection and identification.

counterparts, they have a much richer structure and typically require multivariate statistical decision making procedures. The univariate response signal $y[t]$ of Eq. 6 is replaced by an s -variate vector², hence the VAR(na) model is of the following form:

$$\mathbf{y}[t] + \sum_{i=1}^{na} \mathbf{A}_i \cdot \mathbf{y}[t-i] = \mathbf{e}[t], \quad \text{with} \quad (9)$$

$$\mathbf{e}[t] \sim \text{iid } N(\mathbf{0}, \Sigma), \quad \Sigma = E\{\mathbf{e}[t] \cdot \mathbf{e}^T[t]\}$$

with \mathbf{A}_i ($s \times s$) designating the i -th AR matrix, $\mathbf{e}[t]$ ($s \times 1$) the model residual sequence characterized by the non-singular and generally non-diagonal covariance matrix Σ , n the AR order, and $E\{\cdot\}$ statistical expectation. Given the attitude signal measurements $y[t]$ ($t = 1, 2, \dots, N$), the estimation of the VAR parameter vector θ comprising all AR matrix elements ($\theta = \text{vec}([\mathbf{A}_1 \mathbf{A}_2 \dots \mathbf{A}_{na}])$) and the residual covariance matrix Σ is accomplished via linear regression schemes based on minimization of the Ordinary Least Squares (OLS) or the Weighted Least Squares (WLS) criterion (Refs. 15, 16). The modeling procedure involves the successive fitting of VAR(na) models for increasing AR order n , until an adequate model is achieved. The model order is chosen by replacing the variance of residuals for scalar case by the trace of the residual covariance matrix Σ (Ref. 7).

RESIDUAL BASED FAULT DETECTION

Model residual based methods use functions of the residual sequences (known as characteristic quantity) for fault detection, which are obtained by driving the current signal(s) (Z_u) through the model(s) estimated in the baseline phase for the healthy aircraft, denoted by M_o . The key idea is that the residual sequence obtained by a healthy model that truly reflects the healthy aircraft properties possesses certain distinct properties which are distinguishable from the faulty states of the aircraft.

²Bold-face upper/lower case symbols designate matrix/column-vector quantities, respectively. Matrix transposition is indicated by the superscript T .

The residual series obtained by driving the *current signal(s)* through the aforementioned model is denoted as $e_{ou}[t]$ and is characterized by variance, σ_{ou}^2 . The residual series obtained using *healthy baseline* data records are designated as $e_{oo}[t]$, characterized by variance σ_{oo}^2 .

Residual Variance Method

In this method, the characteristic quantity used for fault detection is the residual variance (Ref. 6). Fault detection is based on the fact that the residual series $e_{ou}[t]$, obtained by driving the current signals, Z_u through the model, M_o (corresponding to the healthy state) should be characterized by variance $\sigma_{ou}^2 = \sigma_{oo}^2$ which becomes minimal if and only if the current state of the aircraft is healthy ($Z_u = Z_o$). Fault detection is based on the following hypothesis testing procedure:

$$H_0 : \sigma_{ou}^2 \leq \sigma_{oo}^2 \quad (\text{null hypothesis - healthy aircraft}) \quad (10)$$

$$H_1 : \sigma_{ou}^2 > \sigma_{oo}^2 \quad (\text{alternate hypothesis - rotor failure})$$

Under the null (H_o) hypothesis, the residuals $e_{ou}[t]$ are (just like the residuals $e_{oo}[t]$), iid Gaussian with zero mean and variance σ_{oo}^2 . Hence the quantities $N_u \cdot \hat{\sigma}_{ou}^2 / \sigma_{oo}^2$ and $(N_o - d) \cdot \hat{\sigma}_{oo}^2 / \sigma_{oo}^2$ follow central χ^2 distribution with N_u and $N_o - d$ degrees of freedom, respectively (as sums of squares of independent standardized Gaussian random variables)³. N_o and N_u designate the number of samples used in estimating the residual variance in the healthy and current cases, respectively (typically $N_o = N_u = N$), and d designates the dimensionality of the estimated model parameter vector. N_u and N_o should be adjusted to $N_u - 1$ and $N_o - 1$, respectively, if each estimated mean is subtracted from each residual sequence. Consequently, the following statistic follows a Fischer distribution (denoted by F) with $(N_u, N_o - d)$ degrees of freedom as

³A hat designates estimator/estimate of the indicated quantity; for instance $\hat{\sigma}$ is an estimator/estimate of σ .

the ratio of two independent and normalized χ^2 random variables (Ref. 6):

$$\text{Under } H_0 : F = \frac{N_u \hat{\sigma}_{ou}^2}{(N_o - d) \hat{\sigma}_{oo}^2} = \frac{\hat{\sigma}_{ou}^2}{\hat{\sigma}_{oo}^2} \quad (11)$$

The following hypothesis test is thus constructed at the α type I (false alarm) risk level:

$$\begin{aligned} F \leq f_{1-\alpha}(N_u, N_o - d) &\Rightarrow H_0 \text{ accepted (healthy aircraft)} \\ \text{Else} &\Rightarrow H_1 \text{ accepted (rotor failure)} \end{aligned} \quad (12)$$

where, $f_{1-\alpha}(N_u, N_o - d)$ designates the corresponding Fischer distribution's $(1 - \alpha)$ critical point.

Residual Uncorrelatedness Method

This method is based on the fact that the residual series $e_{ou}[t]$, obtained by driving the current signals (Z_u) through the model (M_0), is uncorrelated (white) if and only if the aircraft is currently in its healthy condition (Ref. 6). Fault detection is performed by the following hypothesis testing:

$$\begin{aligned} H_0 &: \rho[\tau] = 0 \quad (\text{null hypothesis - healthy aircraft}) \\ H_1 &: \rho[\tau] \neq 0 \quad (\text{alternate hypothesis - rotor failure}) \end{aligned} \quad (13)$$

where $\rho[\tau]$ is the normalized autocorrelation function ($\rho_{xx}[\tau] = \gamma_{xx}[\tau]/\gamma_{xx}[0]$) of the residual sequence $e_{ou}[t]$.

Therefore, the characteristic quantity for fault detection by this method is $[\rho[1] \ \rho[2] \ \rho[3] \ \dots \ \rho[\tau]]^T$. For this method, r is the design variable for the statistical test, which denotes the maximum lag in time (τ) for which the normalized ACFs are being accounted for. Under the null hypothesis (H_0), the residuals $e_{ou}[t]$ are iid Gaussian with zero mean and the test statistic χ_p^2 follows a χ^2 distribution with r degrees of freedom, given as:

$$\text{Under } H_0 : \chi_p^2 = N(N+2) \cdot \sum_{\tau=1}^r (N-\tau)^{-1} \cdot \hat{\rho}[\tau]^2 \sim \chi^2(r) \quad (14)$$

where $\hat{\rho}[\tau]$ denotes the estimator of $\rho[\tau]$.

Statistical decision making is achieved by the following test for α (false alarm) risk level:

$$\begin{aligned} \chi_p^2 \leq \chi_{1-\alpha}^2(r) &\Rightarrow H_0 \text{ is accepted (healthy aircraft)} \\ \text{Else} &\Rightarrow H_1 \text{ is accepted (rotor failure)} \end{aligned} \quad (15)$$

where $\chi_{1-\alpha}^2(r)$ denotes the χ^2 distribution's $1 - \alpha$ critical point.

Sequential Probability Ratio Test

This method employs the Sequential Probability Ratio Test (Refs. 19, 20) in order to detect a change in the standard deviation σ_{ou} of the model residual sequence $e_{ou}[t]$. The SPRT

allows for the specification of two values σ_o and σ_1 for the standard deviation, such that the aircraft is determined to be healthy if and only if $\sigma \leq \sigma_o$, and in faulty state if and only if $\sigma \geq \sigma_1$. The zone between σ_o and σ_1 constitutes an *uncertainty zone*, if any σ is found in this range the decision is postponed and data or residual collection continues. The values of σ_o and σ_1 are user defined and express the increase of the standard deviation in terms of the ratio $q = \frac{\sigma_1}{\sigma_o}$ for which the system is considered to be faulty. For example, a ratio of $q = 1.1$ means that the aircraft is considered faulty whenever there is an increase of 10% in the standard deviation of the current residual sequence compared to a threshold value σ_o .

The SPRT based method leverages both α (false alarm) and β (missed faults) error probabilities in its design. Fault detection is based on the SPRT of strength (α, β) for the following hypothesis testing problem:

$$\begin{aligned} H_0 &: \sigma_{ou} \leq \sigma_0 \quad (\text{null hypothesis - healthy aircraft}) \\ H_1 &: \sigma_{ou} \geq \sigma_1 \quad (\text{alternate hypothesis - rotor failure}) \end{aligned} \quad (16)$$

where σ_{ou} denotes the standard deviation of the residual signal $e_{ou}[t]$ obtained by driving the current signal(s) through the healthy aircraft model, and σ_0 , σ_1 or their ratio q are user defined values. The basis of the SPRT is the logarithm of the likelihood ratio function based on n ($n \leq N$) samples:

$$\mathcal{L}(n) = \sum_{t=1}^n \ln \frac{f(e_{ou}[t]|H_1)}{f(e_{ou}[t]|H_0)} = n \cdot \ln \frac{\sigma_0}{\sigma_1} + \frac{\sigma_0^2 - \sigma_1^2}{2\sigma_0^2\sigma_1^2} \cdot \sum_{t=1}^n e_{ou}[t]^2 \quad (17)$$

with $f(e_{ou}[t] | H_i)$ designating the probability density function of the residual sequence under hypothesis H_i ($i = 0, 1$).

Statistical decision making is then based on the following test at the (α, β) risk levels:

$$\begin{aligned} \mathcal{L}(n) \leq B &\Rightarrow H_0 \text{ is accepted (healthy aircraft)} \\ \mathcal{L}(n) \geq A &\Rightarrow H_1 \text{ is accepted (rotor failure)} \\ B < \mathcal{L}(n) < A &\Rightarrow \text{no decision made (continue the test)} \end{aligned} \quad (18)$$

where:

$$A = \ln \frac{1-\beta}{\alpha} \quad \text{and} \quad B = \ln \frac{\beta}{1-\alpha} \quad (19)$$

Once a decision is made at a stopping time \hat{n} , the test is continued by resetting $\mathcal{L}(\hat{n}+1)$ to zero and continuing by collecting additional residual samples.

RESULTS AND DISCUSSION

Data Generation

Flight simulation for the hexacopter was performed at 5 m/s forward speed with severe turbulence according to the Dryden model. Figures 4 through 6 show attitude time histories for the hexacopter at 5 m/s forward flight, for cases of rotor 1 failure (red) and rotor 2 failure (green). For the simulation results presented, rotor failure (of either rotor 1 or 2) occurs at $t = 10$ s, indicated by the vertical dashed line.

From Fig. 4, it may be observed that rotor 1 failure results in a larger deviation in the pitch attitude than in the case of

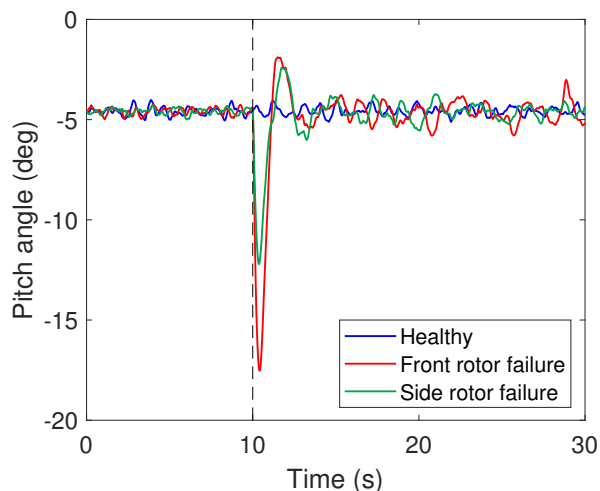


Fig. 4. Indicative pitch attitude signals for an airspeed of 5 m/s. The dashed vertical line indicates the time instant of the fault initiation.

rotor 2 failure. In the case of front rotor failure, the hexacopter pitches down without any substantial change in roll angle (Fig. 5), because the loss of rotor 1 thrust does not significantly affect the aircraft roll equilibrium. However, in the case of side rotor (rotor 2) failure both the pitch (Fig. 4) and roll (Fig. 5) attitudes change and the roll attitude compensation is observed to be underdamped. In Fig. 6, the heading of the aircraft is observed deviating in different directions with the failure of rotor 1 compared to rotor 2. This is due to the different rotor spin directions, and consequently the direction of the hub torque generated by each rotor.

Due to different controller effort for the various levels of turbulence, the aircraft state signals do not show discernible change in characteristics with respect to the healthy dynamics, and transients due to failure and failure compensation under light and moderate levels of turbulence. Similar trends are observed for a flight speed of 10 m/s; the fault detection process follows the same steps for any other speed. In this paper we demonstrate indicative results for a single flight speed of 5 m/s while results from various speeds will be presented in a subsequent publication.

Non-parametric Identification

The STFT-based non-parametric identification of the aircraft dynamics was based on 60 s ($N = 6000$ samples; original signal downsampled to 100 Hz) signals obtained from the aircraft states, namely the translational and rotational position and velocities at 5 m/s forward speed under severe levels of turbulence. Indicative results for pitch signal for healthy and rotor failure (front) analyzed by the Spectrogram or Short Time Fourier Transform (STFT) technique are depicted in Fig. 7. The sampling frequency is taken as 100 Hz and Hamming window of 300 samples with an overlap of 90% is used. It can be observed that there is a sharp change of frequency at the time of rotor failure ($t = 10$ s), distinguishable from the spectrogram of the healthy aircraft.

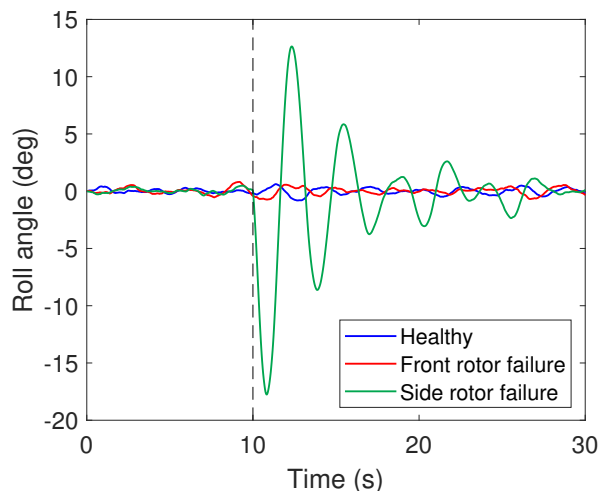


Fig. 5. Indicative roll attitude signals for an airspeed of 5 m/s.

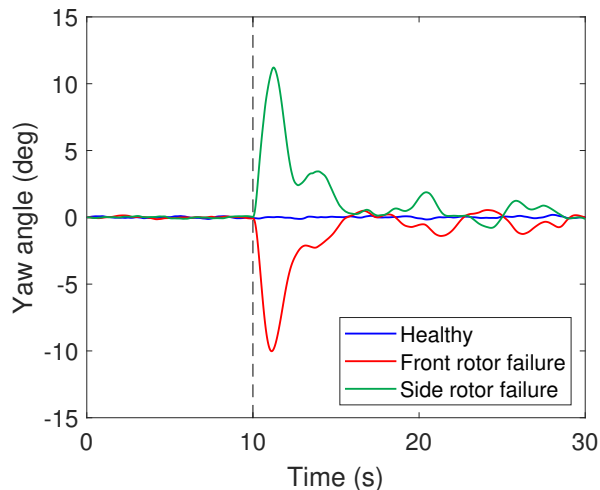


Fig. 6. Indicative yaw attitude signals for an airspeed of 5 m/s.

Scalar AR Identification and Fault Detection

Scalar (univariate) parametric identification of the aircraft dynamics has been based on 20 s ($N = 20000$ samples) of pitch signal obtained from healthy aircraft flight at 5 m/s under severe levels of turbulence. In the present case, the response-only signals have been obtained from ambient excitation due to atmospheric turbulence (assumed to be uncorrelated based on the Dryden specifications). The model parameters and model order, a_i and na , respectively (Eq. 6) need to be estimated so that the model properly represents the dynamics of the system under healthy conditions. The modeling strategy consists of successive fitting of $AR(na)$ models until a suitable model with least amount of complexity (number of parameters) and best fit is selected.

Scalar AR Identification Results

Model order selection is based on a combination of Bayesian Information Criteria (BIC) (Eq. 7) and Residual sum of

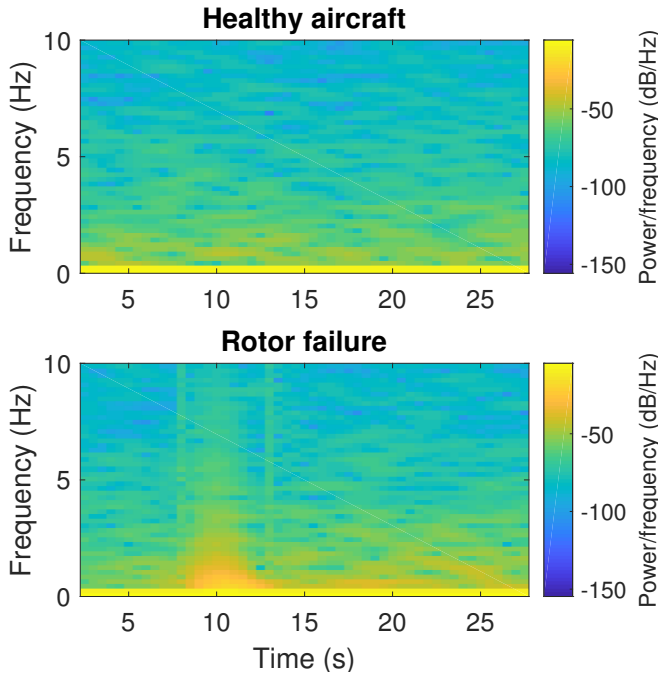


Fig. 7. Spectrogram of the pitch signals under the healthy and front rotor faulty states for a speed of 5 m/s.

squares normalized by Signal sum of squares (RSS/SSS) criteria (Eq. 8) as shown in Fig. 8. A model order of $na = 6$ yields the minimum BIC and this model is represented as AR(6). Monitoring the stabilization of RSS/SSS criteria gives the point where increasing model order does not result further in reduction of prediction errors. This order exhibits a very low RSS/SSS value of $1.6 \times 10^{-10}\%$ demonstrating accurate identification and excellent dynamics representation of the healthy aircraft pitch signal at 5 m/s and under severe turbulence. The number of parameters estimated for the AR(6) model results in a Samples per Parameter (SPP) ratio of 3333.33 ($\frac{N}{7}$).

The model was validated based on the fact that the model matching the current state of the system should generate a white (uncorrelated) residual sequence. Therefore, a healthy pitch signal has been generated from a different realization of severe turbulence. The autocorrelation function of the residual sequences obtained from driving the current signal (healthy) through the model has been observed to be white with 95% confidence (confidence intervals shown in blue), as shown Fig. 9. Next, pitch signals generated under front and side rotor failures have been passed through the same model to generate residual sequences. Figure 9 shows that the residual sequences for different failure cases are serially correlated, demonstrating that the dynamics of the aircraft have changed from that of the healthy state, due to failure.

A similar study has been repeated with the roll and yaw signals to estimate scalar AR models for the healthy aircraft, the details of which are given in Table 2. A comparison of these models using various residual-based fault detection methods will be addressed with respect to their accuracy and ability in detecting faults, as well as their robustness to false alarms.

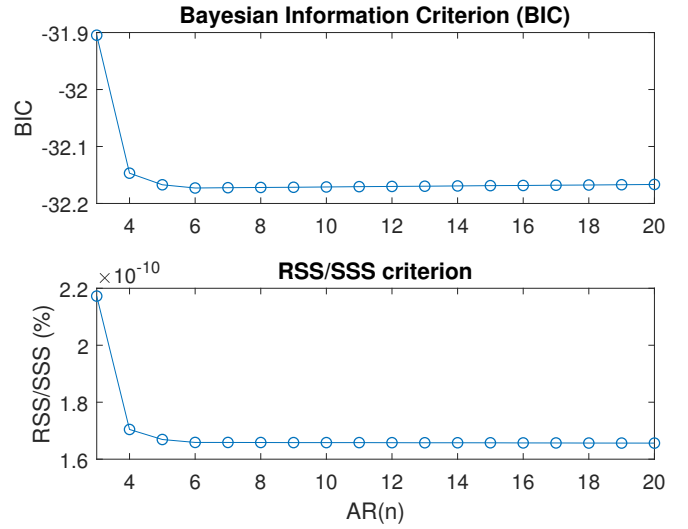


Fig. 8. Scalar AR model order selection criteria.

Residual Based Fault Detection

The current (unknown) pitch signals (5 m/s under severe turbulence) were driven through the identified AR model to generate residual sequences. Fault detection was attempted through the characteristic quantities which are functions of the residual sequences, as previously discussed.

Residual Variance Method

Real-time fault detection is achieved through taking 5 s ($N = 5000$ samples) windows of the current pitch signal at a time with the window being updated every 0.1 s. Then the windowed data are filtered through the estimated healthy model (baseline model) to generate a residual sequence of the same length. The variance of the generated residuals is statistically compared to the corresponding baseline residual variance. The critical limit is determined from the F distribution's $(1 - \alpha)$ critical limit for 5000, 5000-6 degrees of freedom. The hypothesis test is conducted at the α (false alarm) risk level of 10^{-12} and the results for different states of the aircraft (healthy, front, and side rotor failure) are presented in Fig. 10. In all the figures, the vertical black and the horizontal red dashed lines represent the time of rotor failure and the critical limit (threshold), respectively. A fault is detected when the F statistic exceeds the critical limit at the designated type I risk level.

Since a minimum number of 5000 samples are required so that the test is statistically significant with minimum false alarms, the test starts at 5 s. For the current pitch signals coming from a healthy flight, the test statistics (Eq. 10) always remain be-

Table 2. Model identification summary results.

Model Type	Signals used	Model order	Parameters estimated	SPP
Scalar AR	roll	AR(6)	6	3333.33
	pitch	AR(6)	6	3333.33
	yaw	AR(6)	6	3333.33
Vector AR	roll,pitch,yaw	AR(4)	36	166.67

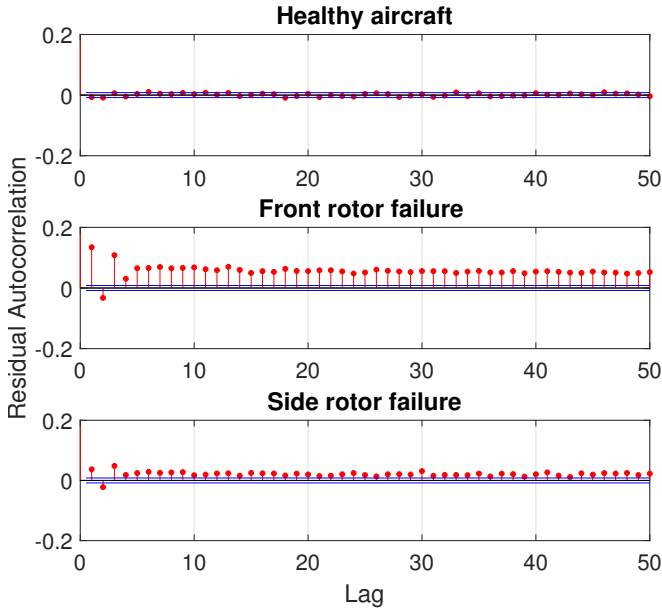


Fig. 9. Autocorrelation function of the pitch residual for the healthy and considered faulty rotor cases.

low the critical limit for the test, hence the null hypothesis (that it is a healthy case) is accepted. In the case of signals generated from an aircraft with rotor failure, the fault detection at the time of failure is immediate, within 0.1 s, which is the window update interval, showing a violation of the critical limit of the test. Thus, the alternate hypothesis of fault is accepted. As observed from the signals in Fig. 4, the pitch signal is affected more for the case of front rotor failure than side rotor failure. Hence, the residual variances for pitch in the case of front rotor failure change more compared to the case side rotor failure, that is also evident from the extent of limit violation of the test statistics. Also, it should be noted that the controller compensates for the fault, returning the pitch dynamics to almost the original state after front rotor failure, as also demonstrated by the test limits receding within the critical limit after the transient signal has passed. However, in the case of side rotor failure, the test statistics continue to cross the critical limit marginally, even after the transient signal has passed, denoting that the pitch dynamics are have been modified with respect to the healthy case. This may be due to the fact that there is strong coupling between pitch and roll control post failure, as side rotor failure causes a large change in the roll axis relative to the front rotor (Fig. 5).

Residual Uncorrelatedness Method

Online fault detection via the residual uncorrelatedness method is performed with the same window length and update interval as discussed in the residual variance method. In these methods, the test statistics (Eq. 13) based on the autocorrelation function of the residuals generated from the current pitch signals are statistically compared to the autocorrelation function of the baseline residuals obtained during the baseline phase. After a preliminary investigation of the effect of the maximum lag τ on the method's performance, a value of 20 has been chosen as adequate. Hence, the $(1 - \alpha)$

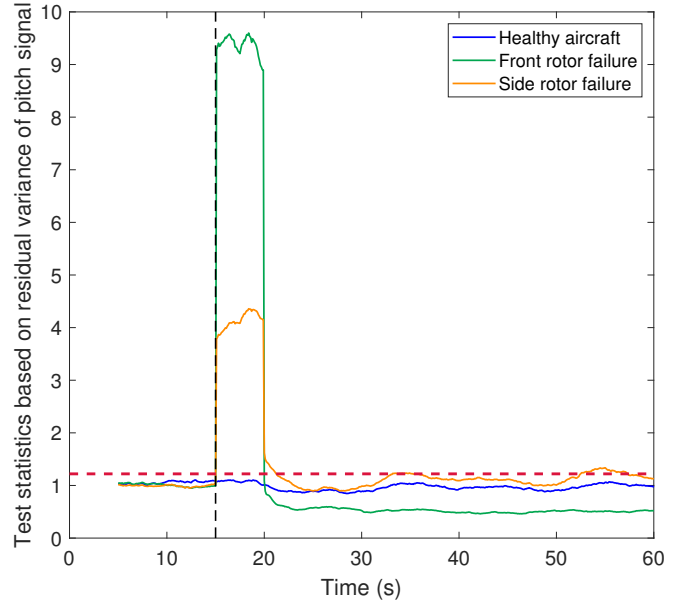


Fig. 10. Indicative pitch residual variance based fault detection results. The dashed red horizontal line indicates the statistical threshold at the $\alpha = 10^{-12}$ risk level. A fault is detected when the test statistic exceeds the threshold.

critical point of a χ^2 distribution with 20 degrees of freedom denotes the critical limit for the statistical hypothesis testing. Figure 11 shows the results for different states of the aircraft for healthy, front and side rotor failure cases, respectively, at the 10^{-3} risk level α . The test statistics crossing over the critical limit (dashed red line) denote rejection of the null hypothesis, thus declaring fault detection. Due to the fault-induced sharp transients in the signals, the fault detection is immediate. Similar to the previous method, due to differences in the pitch signals for front and side rotor failure, the test statistics exceed the critical limit by a greater amount in the former case compared to the latter. Also, due to the controller compensation, the test method is not able to distinguish between healthy and fault compensated pitch signals, as evident from the test statistics going back under the limit in Fig. 11. It should be noted that fault detection is solely based on the response signals; in future work, the controller signals will be also taken into account to differentiate between healthy and fault compensated states of the aircraft and enhance the performance of the methods while taking into account the fault compensation characteristics of the controller.

Sequential Probability Ratio Test

The Sequential Probability Ratio Test (SPRT) method enables online fault detection based on residuals generated from driving the current (unknown) pitch signals through the aforementioned AR model obtained for the healthy state. To implement this technique, an appropriate sampling approach needs to be selected. This involves determination of the following three aspects: (i) the nominal residual standard deviation σ_o for which the aircraft is considered healthy, (ii) the standard deviation ratio $q = \frac{\sigma_1}{\sigma_o}$, which establishes the standard deviation increase under which the aircraft will be considered faulty, and (iii) the

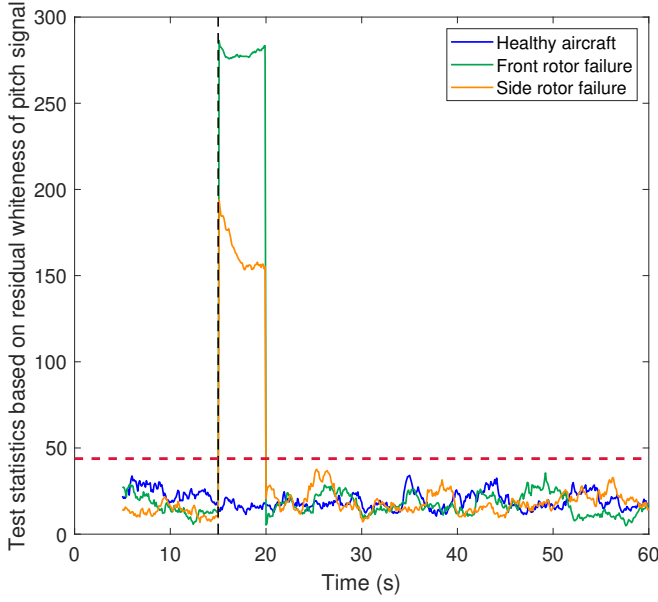


Fig. 11. Indicative pitch residual uncorrelatedness based fault detection results. The dashed red horizontal line indicates the statistical threshold at the $\alpha = 10^{-3}$ risk level.

SPRT strength (α , β).

The residual standard deviation σ_o for which the aircraft is considered healthy is determined based on the 20 available datasets for healthy forward flight at 5 m/s under severe turbulence. From examination of the values of q and (α , β), for minimum false alarms without missing any fault detection these values have been taken as $q = 1.1$ and ($\alpha = 10^{-12}$, $\beta = 10^{-2}$) and the results for different aircraft states have been presented in Fig. 12. The test statistic (blue line) (Eq. 17) exceeding the upper limit denotes a rotor fault, while exceeding the lower limit denotes a healthy aircraft. When the test statistic lies between the two limits, no decision is made and the test continues with using new samples (Eq. 18).

In this method, the number of samples to make a decision is not constant and after a decision is made the SPRT collects new samples until the next decision is made, i.e. the test runs online and decisions are constantly being made with the availability of new data samples. In the case of front rotor failure compensation, the test statistics predict healthy aircraft whereas in the case of side rotor failure, the test continues to detect fault even after the transient has passed. Therefore, the SPRT based on pitch signal is unable to distinguish the aircraft healthy and fault compensated states in some cases. It also signifies that the pitch signal is better compensated to match the healthy aircraft dynamics in the case of front rotor failure compared to side rotor failure.

Vector AR Identification and Fault Detection

Vector (multivariate) parametric identification of the healthy aircraft has been based on 20 s ($N = 2000$ samples at sampling frequency 100 Hz) data sets for the roll, pitch, and yaw signals, without any external excitation (ambient excitation

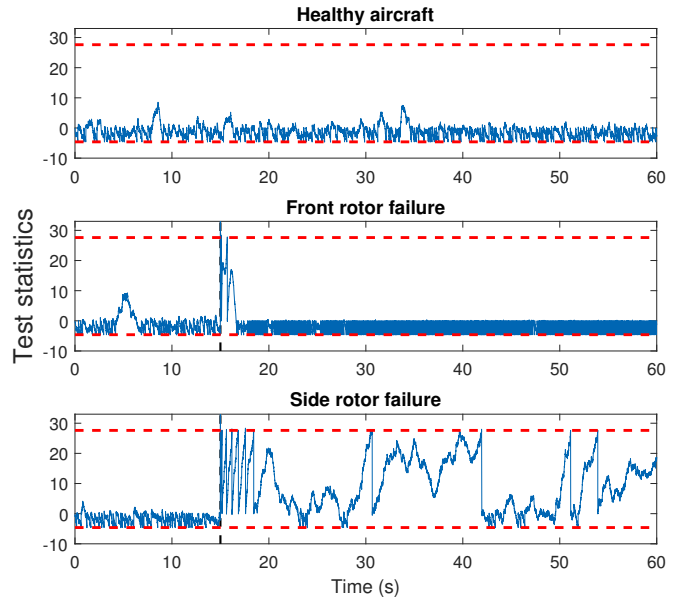


Fig. 12. Indicative results for SPRT based fault detection with pitch signal. The dashed red horizontal lines indicates the critical limits at the $\alpha = 10^{-12}$ and $\beta = 10^{-2}$ risk levels.

due to turbulence assumed to be white) generated from forward flight simulation at 5 m/s under severe turbulence. The model identification follows the same procedure as the scalar model to estimate the parameters a_i and select a model order na which can accurately represent the dynamics of the healthy aircraft.

Model Identification

The model order selection based on the BIC and RSS/SSS criteria yields a model order of 4, represented as VAR(4). The SPP for the model is 166.67 as the number of estimated parameters for VAR(4) is 36 (as the A_i parameter matrix is a 3×3 matrix with $i = 1, 2, 3, 4$ for model order of 4). The roll, pitch and yaw signal of the healthy aircraft flying at 5 m/s for different severe turbulence realization has been driven through the model estimated to generate residuals. The autocorrelation and cross-correlation functions of the three residual sequences generated are observed to be white with 95% confidence. For signals generated for different faulty states, the residuals are found to be correlated. This provides validation of the model, it is capable of representing the dynamics of a healthy aircraft under the considered flight conditions.

VAR Residual Based Fault Detection

The current (unknown) signals (roll, pitch and yaw in that order), when driven through the VAR(4) model estimated in the previous section, yield three sets of residual sequences. The residual based fault detection is performed by the statistical comparison of each characteristic quantity obtained via the current residual sequence with the corresponding quantity obtained via the use of the baseline signals (signal used to

estimate the healthy VAR model) and corresponding residual series through the baseline VAR model. In other words, the characteristic quantity obtained from the current roll residual sequence is compared to the baseline quantity obtained from the roll residual sequence. Therefore, the statistical hypothesis testing is performed thrice for a particular time window (duration of signal measured in number of samples).

Residual Variance Method

The current 5-second-long signals ($N = 500$ samples sampled at 100 Hz frequency), where the window is updated every 0.1s, are driven through the VAR(4) model to generate three sets of residual sequences. Fault detection is achieved through three parallel statistical hypotheses testing of the variance of the current residuals to the variance of the baseline residuals (Eq. 10). The critical limit is determined from the F distribution's $(1 - \alpha)$ critical limit for 500, 500-36 degrees of freedom (because the total number of estimated parameters for the 3-variate VAR(4) model is 36). The statistical hypothesis test is conducted at the α (false alarm) risk level of 10^{-12} to minimize the false alarms and the results for different states of the aircraft are presented in Fig. 13.

To collect a minimum of 500 samples for testing, the test starts from 5 s. For current signals obtained from the healthy flight, the test statistics for each attitude signal fall below the critical limit for the test, denoting acceptance of the null hypothesis. With front and side rotor failure at 10 s, the fault detection, which is evident from all the three test statistics exceeding the critical limit, is immediate. Here, it is interesting to note that the extent of violation is greater in the case of side rotor failure than that for front rotor failure, contrary to the observation in case of scalar AR model of pitch signal only. In the case of side rotor all the three signals (roll, pitch and yaw) change drastically, while in front rotor failure the roll attitude does not change much. As the model captures the correlation between the different signals, the prediction errors are larger for side rotor failure than front rotor failure, as evident from their higher level of crossing the critical limit.

It is also observed that the test statistics for the pitch residual variance recede below the critical limit after the controller has stabilized the system, while the roll and yaw residuals continue to violate the critical limit, which indicates a faulty system. This suggests that the controller compensates for the pitch signal better than the other two attitudes and returns the longitudinal dynamics to a state comparable to that of the healthy aircraft.

Residual Uncorrelatedness Method

Online fault detection by residual uncorrelatedness is performed with 5 s ($N = 500$ samples) window length and update interval of 0.1 s for each residual sequence. In this method, the characteristic quantity is the autocorrelation function of the residuals with a maximum lag $\tau = 20$. The critical limit of the statistical hypothesis testing is given as the $(1 - \alpha)$ critical point of a χ^2 distribution with 20 degrees of freedom. Figure 14 shows three parallel hypothesis tests on roll, pitch and yaw residuals for different current states of the aircraft:

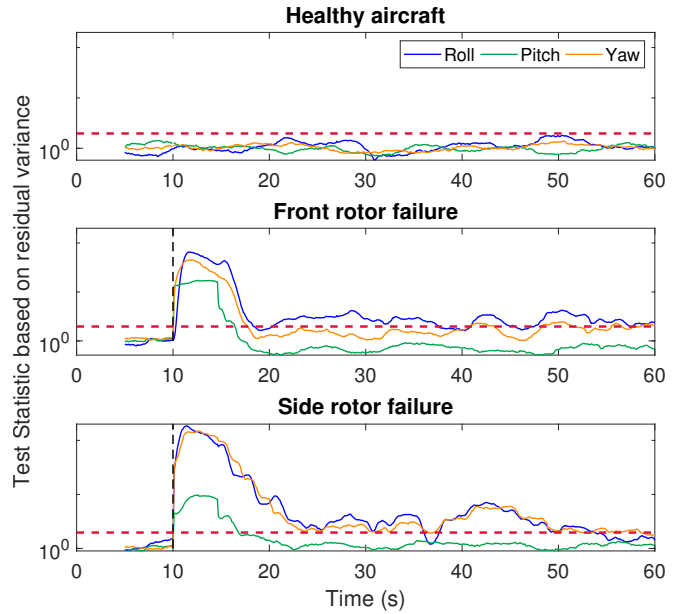


Fig. 13. Indicative residual variance based fault detection results. The dashed red horizontal line indicates the statistical threshold at the $\alpha = 10^{-12}$ risk level.

healthy aircraft, front, and side rotor failure, respectively, at the risk level α of 10^{-3} .

In the healthy case, the test statistic for all the three signals is lower than the the critical limit, correctly declaring the system as healthy. For the front, and side rotor failure at 10 s, fault detection is fast. The test statistics for side rotor failure exceed the critical limit by a greater amount than in case of front rotor failure due to significant change of all three signals in the former compared to only two in the latter, as discussed. Here, post fault compensation, all three test statistics continue to violate the critical limit, indicating a faulty system. Hence, the test is able to distinguish a healthy system from a fault compensated system from the changes in the three attitude signals of the aircraft. It should be noted that the test statistic for roll in the case of side rotor failure shows the maximum deviation, as the controller takes longer time to compensate for it, evident in Fig. 5.

Sequential Probability Ratio Test

The SPRT runs online with the current residuals for roll, pitch and yaw generated from driving the corresponding attitude signals through the VAR(4) model. The appropriate sampling plan to implement this test procedure is different for each of the signals and is determined from the scalar AR modeling of each signal. The value of the variance ratio q is taken to be 1.5, 1.1 and 1.2 for roll, pitch, and yaw, respectively. These values have been decided through rigorous testing to improve false alarms without missing any faults. The nominal residual standard deviation for the attitude signals for which the aircraft is considered healthy are determined based on 20 baseline data sets (generated from simulation of healthy aircraft at 5 m/s under severe turbulence) driven through the baseline model. The strength of SPRT (α , β) is taken as 10^{-12} and 10^{-3} , respectively.

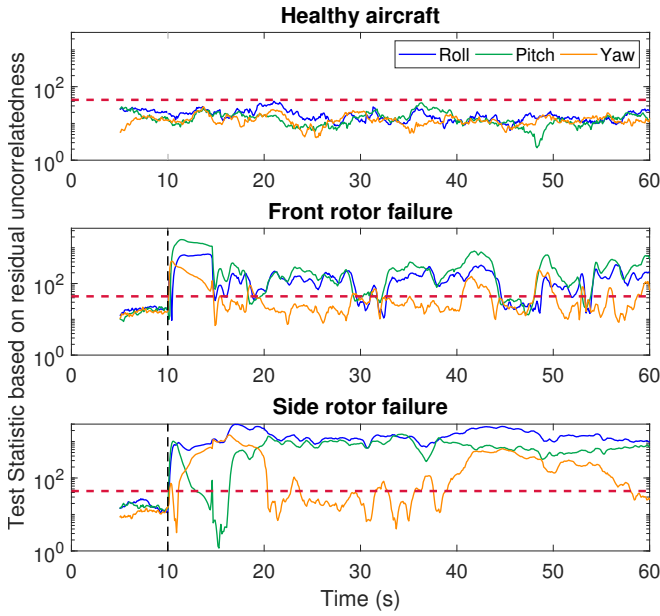


Fig. 14. Indicative residual uncorrelatedness based fault detection results. The dashed red horizontal line indicates the statistical threshold at the $\alpha = 10^{-3}$ risk level.

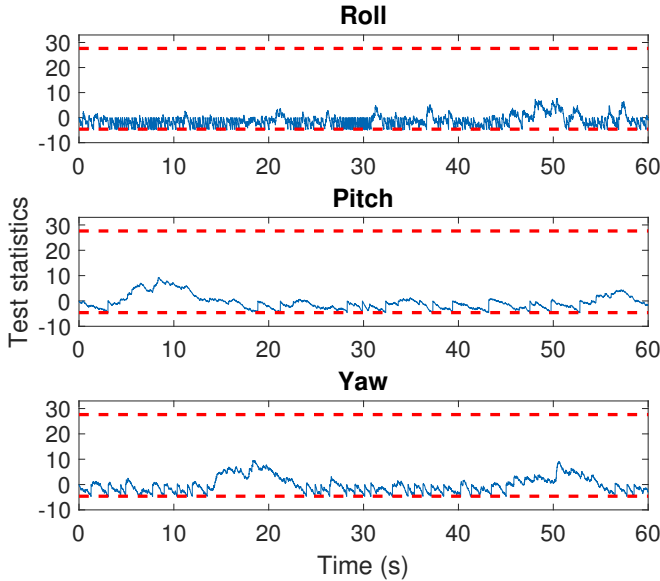


Fig. 15. Indicative results for SPRT method based on the VAR(4) model for healthy aircraft. The dashed red horizontal lines indicate the critical limits at the $\alpha = 10^{-12}$ and $\beta = 10^{-2}$ risk levels.

Indicative fault detection results are presented in Figs. 15 through 17. The aircraft is determined to be in its healthy state when the test statistic exceeds the lower critical point (Fig. 15). Conversely, a fault is detected when the test statistic (vertical axis) exceeds the upper critical point. After a critical point is exceeded, a decision is made, consequently the test statistic is reset to zero and the test continues. Hence, during testing multiple decisions may be made. Evidently, correct detection is obtained in each test case, as the test statistic is shown to exceed multiple times (multiple correct decisions)

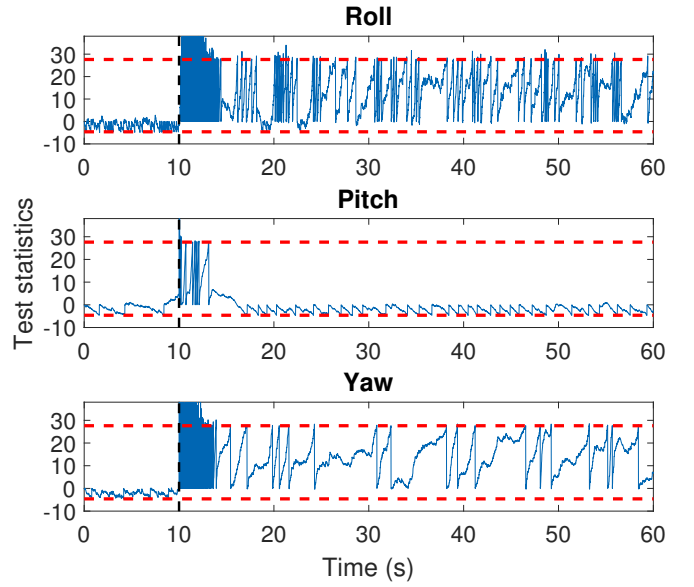


Fig. 16. Indicative results for SPRT method based on the VAR(4) model for front rotor failure. The dashed red horizontal lines indicate the critical limits at the $\alpha = 10^{-12}$ and $\beta = 10^{-2}$ risk levels.

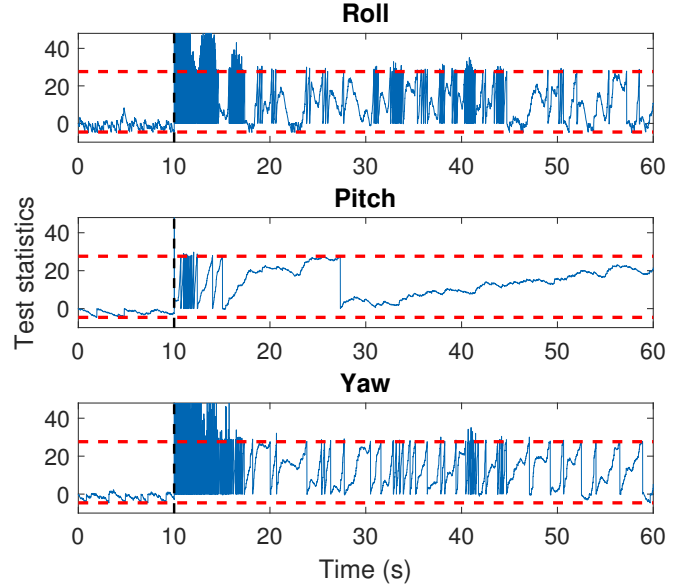


Fig. 17. Indicative results for SPRT based on the VAR(4) model for side rotor failure. The dashed red horizontal lines indicate the critical limits at the $\alpha = 10^{-12}$ and $\beta = 10^{-2}$ risk levels.

the lower critical point in all three signals for the healthy case. The test statistics also exceed the upper critical point multiple times (multiple correct fault detections) in the rotor failure cases, and several observations can be made for the region of post failure failure compensation. The roll and yaw residuals continue to predict faulty state even after the passing of the transient due to rotor failure in all cases. However, the test statistics based on pitch residual settles to the healthy case in front rotor failure, once the fault has been taken care of by the controller (Fig. 16), similar to the results of the scalar AR

Table 3. Parameters used for various fault detection methods

Model type	Fault detection method	Parameters		
		α	β	q
Scalar AR <i>Roll</i>	Residual Variance	$1e-12$	-	-
	Residual Whiteness	$1e-3$	-	-
	SPRT	$1e-12$	$1e-2$	1.5
Scalar AR <i>Pitch</i>	Residual Variance	$1e-12$	-	-
	Residual Whiteness	$1e-3$	-	-
	SPRT	$1e-12$	$1e-2$	1.1
Scalar AR <i>Yaw</i>	Residual Variance	$1e-12$	-	-
	Residual Whiteness	$1e-3$	-	-
	SPRT	$1e-12$	$1e-2$	1.2
Vector AR <i>Roll, Pitch, Yaw</i>	Residual Variance	$1e-12$	-	-
	Residual Whiteness	$1e-3$	-	-
	SPRT	$1e-12$	$1e-2$	1.5, 1.1, 1.2

α : Type I (false alarms) risk level

β : Type II (missed faults) risk level

q : Ratio of residual standard deviation for the system to be considered faulty

pitch signal case (Fig. 12). However, in the case of side rotor failure, this test based on pitch residual is able to distinguish between healthy and fault compensated states (Fig. 17). It is observed that the SPRT method based on the yaw residuals is best suited for distinguishing post failure compensation by the controller as it continues to indicate that the system is faulty unambiguously as opposed to the roll and pitch signals which may indicate a healthy state in this region.

Comparative Assessment of Different Models and Fault Detection Methods

The scalar AR model estimated using the pitch signal of a healthy aircraft flying at a forward speed of 5 m/s under severe level of turbulence exhibits excellent fault detection results with the residual variance and SPRT methods, for current signals obtained from flight at 5 m/s and *all considered levels of turbulence* (light, moderate and severe) (Table 4). The residual uncorrelatedness method is rendered ineffective when the level of turbulence is changed from severe (level for which the model has been estimated) to moderate and light levels. This method shows 100% false alarms for healthy datasets under different levels of turbulence than that used for the model estimation. It should be noted that the forward speed of flight has been held constant at 5 m/s for modeling and validation phase for all cases.

The 3-variate VAR(4) model estimated from the roll, pitch, and yaw signals of the healthy aircraft under the same forward speed and level of turbulence as above, exhibits superior performance than the scalar AR model. The VAR-based methods achieve remarkable results for all levels of turbulence considered in this study (Table 4). In addition, the VAR-based methods have the ability to distinguish between healthy and fault compensated conditions of the aircraft, after the transient dynamics have been compensated by the controller.

With the exception of the scalar AR model estimated using the roll signal, all the fault detection methods can detect rotor

failures within 0.1 s of the event of failure. The scalar methods based on the estimated with roll signal, show a somewhat delayed fault detection (maximum delay being 1.2 s) using the residual variance method and several missed faults using residual uncorrelatedness method for front rotor failure. This is probably due to the fact the roll does not change significantly in this case. On the other hand, the SPRT method does not miss nor shows a delay in detecting front rotor failures using the same scalar model.

The SPRT-based method is able to achieve faster fault detection that is better suited for online application as it uses a smaller number of testing samples than the other methods. In addition, the detection time and number of sample needed for fault detection can be theoretically established and investigated via a well-defined statistical framework (Ref. 9).

Table 3 outlines the different parameters (α, β, q) selected for each residual based fault detection method based on the achieved effectiveness and robustness. If α is not properly adjusted, the method loses efficiency with respect to the probability of false alarms and missed faults. Hence, it is advised to make an initial investigation on the number of false alarms for different levels of turbulence using several healthy data sets. Then, missed fault errors may be checked with data corresponding to various rotor failure states. Moreover, for robust performance of parametric methods, a very small value of the type I risk (α) is often required. This is due to the fact that the stochastic time series models (like AR, ARMA, ARX, state space, etc.) used for modeling the dynamics are still incapable of fully capturing the experimental, operational and environmental uncertainties that the aircraft may be subjected to. Therefore, to “compensate” for the lack of effective uncertainty modeling, a very small α is often selected. Another important factor is the number of samples needed for hypothesis testing, since the chance of missing faults (β) depends upon sample size. For the SPRT method, the values of type I risk (α), type II risk (β), and ratio of residual standard devi-

Table 4. Accuracy of different methods

Model type	Fault detection method	False Alarms %	Missed Rotor Failure		
			Rotor (1)	Rotor (2)	Rotor (6)
Scalar AR <i>Roll</i>	Residual Variance	28.98/15.48/14.57	0/0/0	0/0/0	0/0/0
	Residual Whiteness	3.81/-/-	17/-/-	0/-/-	0/-/-
	SPRT	0.077/0.0025/0	0/0/0	0/0/0	0/0/0
Scalar AR <i>Pitch</i>	Residual Variance	0.082/0/0	0/0/0	0/0/0	0/0/0
	Residual Whiteness	0.61/-/-	0/-/-	0/-/-	0/-/-
	SPRT	0.34/0/0	0/0/0	0/0/0	0/0/0
Scalar AR <i>Yaw</i>	Residual Variance	15.35/2.92/3.59	0/0/0	0/0/0	0/0/0
	Residual Whiteness	10.93/-/-	0/-/-	0/-/-	0/-/-
	SPRT	2.68/1.03/1.09	0/0/0	0/0/0	0/0/0
Vector AR <i>Roll,Pitch,Yaw</i>	Residual Variance	0.045/ 0.49/ 0.25	0/0/0	0/0/0	0/0/0
	Residual Whiteness	0.16 / 0.018 / 0.24	0/0/0	0/0/0	0/0/0
	SPRT	0.065/0/0	0/0/0	0/0/0	0/0/0

False Alarms % for Severe/ Moderate/ Light levels of turbulence

Missed Faults for Severe/ Moderate/ Light levels of turbulence out of 20 datasets each

ation (which gives the increase in standard deviation required to consider the system to be faulty) have been selected carefully to minimize false alarms in healthy signals, but without missing any faults in case of various rotor failures.

CONCLUSIONS

- Statistical time series methods for rotor fault detection in multicopters achieve effective detection based on (i) ambient (white) excitation and aircraft state (*scalar* or *vector*) signals, (ii) statistical model building, and (iii) statistical decision making under uncertainty.
- Both scalar and vector statistical time series methods have shown remarkable results in effectively detecting faults, with the vector methods achieving improved performance with respect to false alarms, missed faults and distinguishing between healthy and faulty compensated states.
- Parametric time series methods are more elaborate and require higher user expertise compared to generally simpler non-parametric approaches like the Spectrogram, but have greater sensitivity to faults and accuracy of detection when fault occurs in real time.
- Vector methods based on a multivariate model are more elaborate, but have the potential of further enhanced performance such as distinction between healthy and fault compensated states from the aircraft states alone, without the knowledge of controller effort. Also, using the difference between autocorrelation and cross-correlation functions of the signal residuals in case of different rotor failures, fault identification is possible.
- The knowledge of controller effort for different levels of turbulence can be used along with the aircraft output to match the performance of simple scalar models with more complex vector models. This can improve their applicability in all levels of turbulence as well as the ability

to distinguish between healthy and post-failure controller compensated states.

- In the future, the modeling will be expanded to Functionally Pooled (FP) model based methods that will include various forward flight speeds and levels of turbulence into a single integrated framework for complete rotor fault detection (abrupt failure and continuous degradation), identification and quantification.

AUTHOR CONTACT

Airin Dutta	duttaa5@rpi.edu
Michael McKay	mckaym2@rpi.edu
Fotis Kopsaftopolous	kopsaf@rpi.edu
Farhan Gandhi	fgandhi@rpi.edu

ACKNOWLEDGEMENT

This work is carried out at Rensselaer Polytechnic Institute under the Army/Navy/NASA Vertical Lift Research Center of Excellence (VLRCE) Program, grant number W911W61120012, with Dr. Mahendra Bhagwat and Dr. William Lewis as Technical Monitors.

REFERENCES

- ¹M. Frangenberg, J. Stephan, and W. Fichter, "Fast Actuator Fault Detection and Reconfiguration for Multicopters," in *AIAA Guidance, Navigation, and Control Conference*, AIAA, Jan. 2015.
- ²G. Heredia and A. Ollera, "Sensor Fault Detection in Small Autonomous Helicopters using Observer/Kalman Filter Identification," in *IEEE International Conference on Mechatronics, Malaga, Spain*, IEEE, Apr. 2009.
- ³M. McKay, R. Niemiec, and F. Gandhi, "Post-Rotor-Failure-Performance of a Feedback Controller for a Hexacopter," in *American Helicopter Society 74th Annual Forum, Phoenix, AZ, AHS*, May 2018.

- ⁴V. Stepanyan, K. Krishnakumar, and A. Bencomo, "Identification and Reconfigurable Control of Impaired Multi-Rotor Drones," in *AIAA Science and Technology Forum and Exposition*, Jan. 2016.
- ⁵X. Qi, D. Theillol, J. Qi, Y. Zhang, and J. Han, "A Literature Review on Fault Diagnosis Methods for Manned and Unmanned Helicopters," in *2013 International Conference on Unmanned Aircraft Systems*, May 2013.
- ⁶S. Fassois and F. Kopsaftopoulos, *New Trends in Structural Health Monitoring*, ch. Statistical Time Series Methods for Vibration Based Structural Health Monitoring, pp. 209–264. Springer, Jan. 2013.
- ⁷F. P. Kopsaftopoulos and S. D. Fassois, "Scalar and Vector Time Series Methods for Vibration Based Damage Diagnosis in a Scale Aircraft Skeleton Structure," *Journal of Theoretical and Applied Mechanics*, vol. 49, no. 4, 2011.
- ⁸P. A. Samara, G. N. Fouskitakis, J. S. Sakellariou, and S. D. Fassois, "A Statistical Method for the Detection of Sensor Abrupt Faults in Aircraft Control Systems," *IEEE Transactions on Control Systems Technology*, vol. 16, pp. 789–798, July 2008.
- ⁹F. P. Kopsaftopoulos and S. D. Fassois, "A vibration model residual-based sequential probability ratio test framework for structural health monitoring," *Structural Health Monitoring*, vol. 14, no. 4, pp. 359–381, 2015.
- ¹⁰D. G. Dimogianopoulos, J. D. Hios, and S. D. Fassois, "FDI for Aircraft Systems Using Stochastic Pooled-NARMAX Representations: Design and Assessment," vol. 17, pp. 1385–1397, Nov. 2009.
- ¹¹D. Peters and C. He, "A Finite-State Induced Flow Model for Rotors in Hover and Forward Flight," in *American Helicopter Society 43rd Annual Forum, St. Louis, MO*, AHS, May 1987.
- ¹²T. M. I. Hakim and O. Arifianto, "Implementation of Dryden Continuous Turbulence Model into Simulink for LSA-02 Flight Test Simulation," in *Journal of Physics: Conference Series 1005(2018) 012017*, Aug. 2018.
- ¹³E. L. Lehmann and J. P. Romano, *Testing Statistical Hypotheses*. Springer, 3rd ed., 2008.
- ¹⁴G. E. P. Box, G. M. Jenkins, and G. C. Reinsel, *Time Series Analysis: Forecasting & Control*. Prentice Hall: Englewood Cliffs, NJ, third ed., 1994.
- ¹⁵L. Ljung, *System Identification: Theory for the User*. Prentice–Hall, 2nd ed., 1999.
- ¹⁶S. D. Fassois, "Parametric identification of vibrating structures," in *Encyclopedia of Vibration* (S. Braun, D. Ewins, and S. Rao, eds.), pp. 673–685, Academic Press, 2001.
- ¹⁷T. Söderström and P. Stoica, *System Identification*. Prentice–Hall, 1989.
- ¹⁸H. Lütkepohl, *New Introduction to Multiple Time Series Analysis*. Springer-Verlag Berlin, 2005.
- ¹⁹A. Wald, *Sequential Analysis*. New York: Dover Publications Inc., 2004.
- ²⁰B. K. Ghosh and P. K. Sen, eds., *Handbook of Sequential Analysis*. New York: Marcel Dekker, Inc., 1991.